Energy-stable numerical schemes for multiscale simulations of polymer-solvent mixtures *

M. Lukáčová-Medviďová, B. Dünweg, P. Strasser, N. Tretyakov

Abstract We present a new second order energy dissipative numerical scheme to treat macroscopic equations aiming at the modeling of the dynamics of complex polymer-solvent mixtures. These partial differential equations are the Cahn-Hilliard equation for diffuse interface phase fields and the Oldroyd-B equations for the hydrodynamics of the polymeric mixture. A second order combined finite volume / finite difference method is applied for the spatial discretization. A complementary approach to study the same physical system is realized by simulations of a microscopic model based on a hybrid Lattice Boltzmann / Molecular Dynamics scheme. These latter simulations provide initial conditions for the numerical solution of the macroscopic equations. This procedure is intended as a first step towards the development of a multiscale method that aims at combining the two models.

1 Introduction

Phase separation in binary fluids is a fundamental process in condensed-matter physics. For Newtonian fluids the phenomenon of spinodal decomposition is reasonably well understood in terms of the so-called "model H" [10, 3, 15], where

M. Lukáčová-Medvid'ová
Institute of Mathematics, University of Mainz, e-mail: lukacova@uni-mainz.de

B. Dünweg
Max Planck Institute for Polymer Research, Mainz, e-mail: duenweg@mpip-mainz.mpg.de

P. Strasser
Institute of Mathematics, University of Mainz, e-mail: strasser@uni-mainz.de

N. Tretyakov
Max Planck Institute f. Polymer Research, Mainz, e-mail: tretyakov@mpip-mainz.mpg.de

* The present paper has been supported by the German Science Foundation (DFG) under the grant TRR 146.

the hydrodynamic equations of motion for mass and momentum conservation are coupled to a convection-diffusion equation for the concentration (or in general the "phase field" variable ϕ), and the thermodynamics, which is described by a (free) energy functional $E(\phi)$, gives rise to a driving force, see, e.g., [1, 19, 9, 21]. In such "diffuse interface" or "phase field" models, the interface between two phases is a thin layer of finite thickness, across which ϕ varies continuously. A big advantage of such models is that interfaces are defined implicitly and do not need to be tracked. Similarly, topological changes of the interface structure are automatically described correctly. However, phase field models are generally very challenging to solve numerically.

The physics (and therefore also the mathematics and numerics) becomes much more involved if one component — or both — is a macromolecular compound. In this case, the large molecular relaxation time gives rise to a dynamic coupling between intra-molecular processes and the unmixing on experimentally relevant time scales, with interesting new phenomena, for which the term "viscoelastic phase separation" [18] has been coined. Here the construction of physically sound dynamic equations with suitable constitutive relations to describe the viscoelasticity is already a challenge in itself. *Tanaka* [18] made the first attempt in this direction; however, *Zhou et al.* [21] showed later that this dynamics violates the second law of thermodynamics and provided a corrected set of equations that satisfy it. Nevertheless, a fully satisfactory solution of the problem is probably still missing. For this reason, we wish to carefully investigate how well this system describes the physics, by comparing it with and linking it to a computer experiment that is based upon a microscopic (molecular) model (see Sec. 4) that can be considered as physically sound beyond reasonable doubt. We thus study the diffuse-interface viscoelastic equations put forward in [21] for the case of the unmixing process of a polymer-solvent system.

Typically the interfacial region separating the two fluids is very narrow, and a high spatial resolution is required to accurately capture the interface dynamics. In fact, the underlying problem is stiff, which necessitates an implicit time discretization. Moreover, the solution admits several time scales over which it evolves, cf. [12]. In the literature one can find already several numerical methods that have been used for the numerical approximation of diffuse interface models, see, e.g., [4, 9, 12, 13, 19] and the references therein.

In order to describe the dynamics of a complex polymer-solvent mixture, the Cahn-Hilliard equations for the phase field evolution are coupled with the Oldroyd-B equations, which consist of the momentum equation for the velocity field, the continuity equation, and the rheological equation for time evolution of the elastic stress tensor. We note in passing that there is quite a large number of analytical as well as numerical results available in the literature for the Oldroyd-B system, see, e.g., [2, 6, 7, 14]. The main challenge in this field is to obtain a stable approximate numerical solution for large Weissenberg numbers. The dimensionless Weissenberg number represents elastic effects; it is large when the molecular relaxation time is comparable to the time scale of the flow, or even exceeds it significantly. In the present work we consider the non-critical regime of Weissenberg numbers. Apply-

ing the techniques from [6, 14], a further generalization using the log-transformation of the elastic stress tensor and the Lagrange-type approximation of the convective term is possible.

2 Mathematical Model

Following *Zhou, Zhang & E* [21] the total energy of the polymer-solvent mixture consists of the mixing, the polymerization, the elastic and the kinetic energy:

$$\begin{aligned} E_{tot}(\phi,q,\sigma,\mathbf{u}) &= E_{mix}(\phi)+E_{pol}(q)+E_{el}(\sigma)+E_{kin}(\mathbf{u}) \\ &= \int_\Omega \left(\frac{C_0}{2}|\nabla\phi|^2+F(\phi)\right)+\int_\Omega \frac{1}{2}|q|^2+\int_\Omega \frac{1}{2}\mathrm{tr}(\sigma)+\int_\Omega \frac{1}{2}|\mathbf{u}|^2. \end{aligned} \quad (1)$$

Here ϕ is the volume fraction of polymer molecules, q the bulk stress, σ the elastic shear stress tensor and $\mathbf{u}$ the volume averaged velocity. Furthermore, C_0 is a positive constant and $F(\phi)$ denotes a double-well potential. In the present paper we work with the logarithmic potential derived from standard Flory-Huggins theory [16]

$$F(\phi)=\frac{1}{n_p}\phi\ln\phi+\frac{1}{n_s}(1-\phi)\ln(1-\phi)+\chi\phi(1-\phi) \quad (2)$$

with n_p and n_s the molecular weight of the two components (p: polymer, s: solvent) and $\chi=\chi_0/T$ the effective Flory interaction which depends on the temperature T. Consequently, $\phi\in[0,1]$.

Following standard procedures in non-equilibrium thermodynamics *Zhou et al.* [21] split the currents into a reversible and a nonreversible part. The reversible contributions are obtained through the virtual work principle, while the irreversible contributions are obtained by analyzing the dissipative process. The corresponding dynamic model then reads

$$\begin{aligned} \frac{\partial\phi}{\partial t}+\mathbf{u}\cdot\nabla\phi &= \nabla\cdot\left\{\phi(1-\phi)M\left[\phi(1-\phi)\nabla\mu-\nabla(A_1(\phi)q)\right]\right\}, \\ \frac{\partial q}{\partial t}+\mathbf{u}\cdot\nabla q &= -\frac{1}{\tau(\phi)}q-A_1(\phi)\nabla\cdot\left\{M\left[\phi(1-\phi)\nabla\mu-\nabla(A_1(\phi)q)\right]\right\}, \\ \frac{\partial\sigma}{\partial t}+(\mathbf{u}\cdot\nabla)\sigma &= (\nabla\mathbf{u})\cdot\sigma+\sigma\cdot(\nabla\mathbf{u})^T-\frac{1}{\tau_s(\phi)}\sigma+B_2(\phi)\left[\nabla\mathbf{u}+(\nabla\mathbf{u})^T\right], \\ \frac{\partial\mathbf{u}}{\partial t}+(\mathbf{u}\cdot\nabla)\mathbf{u} &= -\nabla p+\nabla\cdot\left\{\eta(\phi)\left[\nabla\mathbf{u}+(\nabla\mathbf{u})^T\right]\right\}+\mu\nabla\phi+\nabla\cdot\sigma, \\ \nabla\cdot\mathbf{u} &= 0, \end{aligned} \quad (3)$$

where $M > 0$ is the mobility coefficient, $\tau(\phi) = \tau^0 \phi^2$ and $\tau_s(\phi) = \tau_s^0 \phi^2$ are the relaxation times, $B_2(\phi) = m_s^0 \phi^2$ is the relaxation modulus, $A_1(\phi) \in [1,2]$ is the bulk modulus, $\eta(\phi) \in [0,1]$ is the viscosity and all relaxation coefficients are positive. Furthermore, p denotes the pressure and μ, the chemical potential, is given by

$$\mu = \frac{\delta E_{mix}(\phi)}{\delta \phi} = -C_0 \Delta \phi + F'(\phi). \tag{4}$$

This model is thermodynamically consistent and dissipates energy over time if $\mathrm{tr}(\sigma) > 0$. The latter holds true at any time, if the determinant of the initial value of the so-called conformation tensor $\mathbf{c}$ is greater than one, see *Hu & Lelièvre* [11]. Here $\mathbf{c}$ is defined as $\mathbf{c} := \frac{1}{B_2(\phi)}\sigma + \mathbb{1}$, where $\mathbb{1}$ is the identity matrix.

Theorem 1. *The problem* (3) *satisfies the following energy law*

$$\frac{dE_{tot}(\phi,q,\sigma,\mathbf{u})}{dt} + \frac{1}{\tau^0}\left\|\frac{q}{\phi}\right\|^2_{L^2(\Omega)} + \int_\Omega M\Big[\phi(1-\phi)\nabla\mu - \nabla(A_1(\phi)\,q)\Big]^2 + \int_\Omega \frac{1}{2\,\tau_s(\phi)}\mathrm{tr}(\sigma) + \int_\Omega \frac{\eta(\phi)}{2}\sum_{i,j}\left(\frac{\partial u_i}{\partial x_j} + \frac{\partial u_j}{\partial x_i}\right)^2 = 0. \tag{5}$$

Proof. Multiplying $(3)_1$ by μ and integrating over the computational domain Ω, assuming suitable boundary conditions (e.g. periodic boundary conditions), and applying integration by parts, we obtain

$$\begin{aligned}
&\int_\Omega \frac{\partial \phi}{\partial t}\mu + \int_\Omega \mathbf{u}\cdot\nabla\phi\mu - \int_\Omega \nabla\cdot\Big\{\phi(1-\phi)M\Big[\phi(1-\phi)\nabla\mu - \nabla(A_1(\phi)\,q)\Big]\Big\}\mu \\
&= \int_\Omega \frac{\partial \phi}{\partial t}\frac{\delta E_{mix}(\phi)}{\delta\phi} + \int_\Omega \mathbf{u}\cdot\nabla\phi\mu + \int_\Omega \Big\{\phi(1-\phi)M\Big[\phi(1-\phi)\nabla\mu - \nabla(A_1(\phi)\,q)\Big]\Big\}\nabla\mu \\
&= \frac{dE_{mix}(\phi)}{dt} + \int_\Omega \mathbf{u}\cdot\nabla\phi\mu + \int_\Omega M\Big[\phi(1-\phi)\nabla\mu - \nabla(A_1(\phi)\,q)\Big]\Big[\phi(1-\phi)\nabla\mu\Big] = 0.
\end{aligned}$$

Now, using the previously explained procedure after multiplying $(3)_2$ by q, and making use of $\nabla\cdot\mathbf{u} = 0$ yield

$$\int_\Omega \frac{\partial q}{\partial t} q + \int_\Omega \mathbf{u}\cdot\nabla q q + \int_\Omega \frac{1}{\tau(\phi)} q^2 + \int_\Omega A_1(\phi)\nabla\cdot\Big\{M\Big[\phi(1-\phi)\nabla\mu - \nabla(A_1(\phi)\,q)\Big]\Big\}\,q$$
$$= \int_\Omega \frac{1}{2}\frac{\partial}{\partial t} q^2 + \frac{1}{2}\int_\Omega \mathbf{u}\cdot\nabla q^2 + \int_\Omega \frac{1}{\tau^0\phi^2} q^2$$
$$+ \int_\Omega \nabla\cdot\Big\{M\Big[\phi(1-\phi)\nabla\mu - \nabla(A_1(\phi)\,q)\Big]\Big\} A_1(\phi)\,q$$
$$= \frac{d}{dt}\left(\int_\Omega \frac{1}{2} q^2\right) - \frac{1}{2}\int_\Omega \nabla\cdot\mathbf{u}\, q^2 + \frac{1}{\tau^0}\left\|\frac{q}{\phi}\right\|^2_{L^2(\Omega)}$$
$$- \int_\Omega M\Big[\phi(1-\phi)\nabla\mu - \nabla(A_1(\phi)\,q)\Big]\nabla(A_1(\phi)\,q)$$
$$= \frac{dE_{pol}(q)}{dt} + \frac{1}{\tau^0}\left\|\frac{q}{\phi}\right\|^2_{L^2(\Omega)} + \int_\Omega M\Big[\phi(1-\phi)\nabla\mu - \nabla(A_1(\phi)\,q)\Big]\Big[-\nabla(A_1(\phi)\,q)\Big] = 0\,.$$

For the next step we remind that for all $A\in\mathbb{R}^{n\times n},\ n\in\mathbb{N}$: $\operatorname{tr}(\mathbf{A}) = \operatorname{tr}(\mathbf{A}\cdot\mathbb{1}^T) = \mathbf{A}:\mathbb{1}$. Hence, applying the aforementioned computational steps after multiplying $(3)_3$ by $\frac{1}{2}\mathbb{1}$ implies

$$\int_\Omega \frac{1}{2}\operatorname{tr}\left(\frac{\partial\sigma}{\partial t}\right) + \int_\Omega \frac{1}{2}\operatorname{tr}((\mathbf{u}\cdot\nabla)\sigma) - \int_\Omega \frac{1}{2}\left(\nabla\mathbf{u} : \sigma^T + \sigma : \nabla\mathbf{u}\right) + \int_\Omega \frac{1}{2\,\tau_s(\phi)}\operatorname{tr}(\sigma)$$
$$- \int_\Omega B_2(\phi)\operatorname{tr}(\nabla\mathbf{u})$$
$$= \int_\Omega \frac{1}{2}\frac{\partial}{\partial t}\operatorname{tr}(\sigma) - \int_\Omega \frac{1}{2}\operatorname{tr}((\nabla\cdot\mathbf{u})\sigma) - \int_\Omega \sigma:\nabla\mathbf{u} + \int_\Omega \frac{1}{2\,\tau_s(\phi)}\operatorname{tr}(\sigma) - \int_\Omega B_2(\phi)(\nabla\cdot\mathbf{u})$$
$$= \frac{d}{dt}\int_\Omega \frac{1}{2}\operatorname{tr}(\sigma) - \int_\Omega \sigma:\nabla\mathbf{u} + \int_\Omega \frac{1}{2\,\tau_s(\phi)}\operatorname{tr}(\sigma) = 0\,.$$

Multiplying $(3)_4$ by $\mathbf{u}$ (scalar product), and again applying the same procedure give

$$\int_\Omega \frac{\partial\mathbf{u}}{\partial t}\cdot\mathbf{u} + \frac{1}{2}\int_\Omega (\mathbf{u}\cdot\nabla)|\mathbf{u}|^2 + \int_\Omega \Big\{\eta(\phi)\Big[\nabla\mathbf{u} + (\nabla\mathbf{u})^T\Big]\Big\} : \nabla\mathbf{u} - \int_\Omega p(\nabla\cdot\mathbf{u})$$
$$- \int_\Omega \mu\nabla\phi\cdot\mathbf{u} - \int_\Omega \nabla\cdot\sigma\cdot\mathbf{u}$$
$$= \int_\Omega \frac{1}{2}\frac{\partial|\mathbf{u}|^2}{\partial t} - \frac{1}{2}\int_\Omega (\nabla\cdot\mathbf{u})|\mathbf{u}|^2 + \int_\Omega \Big\{\eta(\phi)\Big[|\nabla\mathbf{u}|^2 + \operatorname{tr}\left((\nabla\mathbf{u})^2\right)\Big]\Big\}$$
$$- \int_\Omega \mathbf{u}\cdot\nabla\phi\mu + \int_\Omega \sigma:\nabla\mathbf{u}$$
$$= \frac{d}{dt}\int_\Omega \frac{1}{2}|\mathbf{u}|^2 + \int_\Omega \frac{\eta(\phi)}{2}\sum_{i,j}\left(\frac{\partial u_i}{\partial x_j} + \frac{\partial u_j}{\partial x_i}\right)^2 - \int_\Omega \mathbf{u}\cdot\nabla\phi\mu + \int_\Omega \sigma:\nabla\mathbf{u} = 0\,.$$

Summing up all four equations yields the energy law (5). We refer a reader also to [21], where analogous energy dissipation property has stated. □

3 Numerical Scheme

In this section we present a new combined finite volume-finite difference method for the numerical solution of the macroscopic equations (3). We consider a uniform partition of the time interval $[0,T]$ with constant time step size Δt. In the first step we propose to apply a linear second order time discretizaton in order to approximate the crucial phase field variables (ϕ, q) of the Cahn-Hilliard type equations.

Step 1. Find (ϕ^{n+1}, q^{n+1}), such that

$$
\begin{aligned}
&\frac{\phi^{n+1}-\phi^n}{\Delta t} + \tilde{\mathbf{u}}^n \cdot \nabla \tilde{\phi}^n = \nabla \cdot \left\{ \tilde{\phi}^n (1-\tilde{\phi}^n) M \left[\tilde{\phi}^n (1-\tilde{\phi}^n) \nabla \mu^{n+\frac{1}{2}} - \nabla (A_1(\tilde{\phi}^n)\, q^{n+\frac{1}{2}}) \right] \right\},\\
&\mu^{n+\frac{1}{2}} = -C_0 \Delta \phi^{n+\frac{1}{2}} + f(\phi^{n+1}, \phi^n),\\
&\frac{q^{n+1}-q^n}{\Delta t} + \mathbf{u}^n \cdot \nabla q^{n+\frac{1}{2}} =\\
&\quad = -\frac{1}{\tau(\tilde{\phi}^n)} q^{n+\frac{1}{2}} - A_1(\tilde{\phi}^n) \nabla \cdot \left\{ M \left[\tilde{\phi}^n (1-\tilde{\phi}^n) \nabla \mu^{n+\frac{1}{2}} - \nabla (A_1(\tilde{\phi}^n)\, q^{n+\frac{1}{2}}) \right] \right\},
\end{aligned}
\tag{6}
$$

where $\phi^{n+\frac{1}{2}} = \frac{1}{2}(\phi^{n+1}+\phi^n)$ and $q^{n+\frac{1}{2}} = \frac{1}{2}(q^{n+1}+q^n)$. Further,

$$
\tilde{\mathbf{u}}^n := \mathbf{u}^n + \Delta t\, \mu^{n+\frac{1}{2}} \nabla \tilde{\phi}^n, \tag{7}
$$

to split the phase field part from the hydrodynamic part and $\tilde{\phi}^n = \frac{1}{2}(3\phi^n - \phi^{n-1})$ to keep the second order time discretization while staying linear, see *Gonzáles, Tierra* [19]. For the approximation of the derivative of the double-well potential we set

$$
f(\phi^{n+1}, \phi^n) = f(\phi^n) + \frac{1}{2} f'(\phi^n)\,(\phi^{n+1} - \phi^n).
$$

This discretization is the so called optimal dissipation approximation which ensures a second order approximation for smooth phase fields and entropy dissipation [19].

In the second step we approximate the fluid equations as follows.

Step 2. Denote by $D(\mathbf{u}^{n+1}) = \frac{1}{2}\left[\nabla \mathbf{u}^{n+1} + (\nabla \mathbf{u}^{n+1})^T\right]$ the symmetric velocity gradient. Applying the Chorin pressure projection method we find $(\mathbf{u}^{n+1}, p^{n+1})$, such that

$$
\begin{aligned}
&\frac{\mathbf{u}^{n+1}-\tilde{\mathbf{u}}^n}{\Delta t} + (\mathbf{u}^n \cdot \nabla)\mathbf{u}^{n+1} = \nabla \cdot \left\{ \eta(\phi^{n+\frac{1}{2}})\, 2D(\mathbf{u}^{n+1}) \right\} - \nabla p^{n+1} + \nabla \cdot \sigma^n,\\
&\nabla \cdot \mathbf{u}^{n+1} = 0.
\end{aligned}
\tag{8}
$$

Note that (8) yields a first order time implicit discretization. Generalization to higher orders is possible by applying, e.g., the fractional θ-scheme [20].

Finally, in the third step we approximate the Oldroyd-B equation for the time evolution of the viscoelastic stress tensor σ.

Step 3. Find σ^{n+1}, such that

$$\frac{\sigma^{n+1}-\sigma^n}{\Delta t}+(\mathbf{u}^{n+1}\cdot\nabla)\sigma^n=(\nabla\mathbf{u}^{n+1})\cdot\sigma^n-\sigma^n\cdot\left(\nabla\mathbf{u}^{n+1}\right)^T \\ -\frac{1}{\tau_s(\phi^{n+\frac{1}{2}})}\sigma^n+B_2(\phi^{n+\frac{1}{2}})\,2D(\mathbf{u}^{n+1})\,. \tag{9}$$

Theorem 2. *The numerical scheme (6)-(9) is energy stable. More precisely, the scheme satisfies the discrete version of the energy law*

$$\frac{E_{tot}(\phi^{n+1},q^{n+1},\sigma^{n+1},\mathbf{u}^{n+1})-E_{tot}(\phi^n,q^n,\sigma^n,\mathbf{u}^n)}{\Delta t}+\int_\Omega\frac{1}{2\,\tau_s(\phi^{n+\frac{1}{2}})}\mathrm{tr}(\sigma^n) \\ +\int_\Omega\frac{\eta(\phi^{n+\frac{1}{2}})}{2}\sum_{i,j}\left(\frac{\partial u_i^{n+1}}{\partial x_j}+\frac{\partial u_j^{n+1}}{\partial x_i}\right)^2+\frac{1}{\tau^0}\left\|\frac{q^{n+\frac{1}{2}}}{\tilde\phi^n}\right\|^2_{L^2(\Omega)} \tag{10}$$
$$+\int_\Omega M\left[\tilde\phi^n(1-\tilde\phi^n)\nabla\mu^{n+\frac{1}{2}}-\nabla(A_1(\tilde\phi^n)\,q^{n+\frac{1}{2}})\right]^2+ND^{n+1}_{phobic}+ND^{n+1}_{split}=0\,,$$

where

$$ND^{n+1}_{phobic}:=\int_\Omega f(\phi^{n+1},\phi^n)\frac{\phi^{n+1}-\phi^n}{\Delta t}-\int_\Omega\frac{F(\phi^{n+1})-F(\phi^n)}{\Delta t}\,,$$

$$ND^{n+1}_{split}:=\frac{1}{2\Delta t}\left(\|\mathbf{u}^{n+1}-\tilde{\mathbf{u}}^n\|^2_{L^2(\Omega)}+\|\tilde{\mathbf{u}}^n-\mathbf{u}^n\|^2_{L^2(\Omega)}\right).$$

Proof. Similar to the proof of the continuous energy law, we multiply $(6)_1$ by $\mu^{n+\frac{1}{2}}$, $(6)_3$ by $q^{n+\frac{1}{2}}$, $(8)_1$ by $\mathbf{u}^{n+1}$, and (9) by $\frac{1}{2}\mathbb{1}$, and integrate. Assuming suitable boundary conditions, the calculation of the discrete polymeric and elastic energy is analogous to the continuous case. The calculation of the discrete mixing energy leads to the additional terms ND^{n+1}_{phobic} and $\int_\Omega(\tilde{\mathbf{u}}^n\cdot\nabla\tilde\phi^n)\mu^{n+\frac{1}{2}}$. The key point of the splitting scheme lies in the matching of the latter term with $\int_\Omega\frac{1}{\Delta t}(\mathbf{u}^{n+1}-\tilde{\mathbf{u}}^n)\cdot\mathbf{u}^{n+1}$, which arises while calculating the discrete kinetic energy. This is possible by multiplying expression (7) by $\tilde{\mathbf{u}}^n$, and integrating which yield

$$\|\tilde{\mathbf{u}}^n\|^2_{L^2(\Omega)}=\int_\Omega\mathbf{u}^n\cdot\tilde{\mathbf{u}}^n+\int_\Omega\Delta t(\tilde{\mathbf{u}}^n\cdot\nabla\tilde\phi^n)\mu^{n+\frac{1}{2}}\,.$$

This implies

$$\int_\Omega (\tilde{\mathbf{u}}^n \cdot \nabla \tilde{\phi}^n)\mu^{n+\frac{1}{2}} = \frac{1}{\Delta t}\left(\|\tilde{\mathbf{u}}^n\|^2_{L^2(\Omega)} - \int_\Omega \mathbf{u}^n \cdot \tilde{\mathbf{u}}^n \right)$$
$$= \frac{1}{2\Delta t}\left(\|\tilde{\mathbf{u}}^n\|^2_{L^2(\Omega)} - \|\mathbf{u}^n\|^2_{L^2(\Omega)} + \|\tilde{\mathbf{u}}^n - \mathbf{u}^n\|^2_{L^2(\Omega)} \right),$$

since

$$\int_\Omega \frac{1}{\Delta t}(\mathbf{u}^{n+1} - \tilde{\mathbf{u}}^n)\cdot \mathbf{u}^{n+1} = \frac{1}{2\Delta t}\left(\|\mathbf{u}^{n+1}\|^2_{L^2(\Omega)} - \|\tilde{\mathbf{u}}^n\|^2_{L^2(\Omega)} + \|\mathbf{u}^{n+1} - \tilde{\mathbf{u}}^n\|^2_{L^2(\Omega)} \right).$$

In conclusion we obtain the discrete energy law (10) and consequently

$$E_{tot}(\phi^{n+1}, q^{n+1}, \sigma^{n+1}, \mathbf{u}^{n+1}) \leq E_{tot}(\phi^n, q^n, \sigma^n, \mathbf{u}^n), \tag{11}$$

provided that we control ND^{n+1}_{phobic}, since all other terms are non-negative. In [9] it has been shown that $ND^{n+1}_{phobic} = \mathscr{O}(\Delta t^2)$. Our numerical experiments presented below indeed confirm that the energy dissipation (11) holds. □

Let us note that the computational domain $\Omega \subset \mathbb{R}^2$ is discretized by a regular rectangular grid. The discretization in space is realized by a finite volume scheme using second order upwinding for the convective terms and central differences for the remaining terms.

4 Lattice Boltzmann and Molecular Dynamics Simulation

Starting point of the simulation model is a standard Kremer-Grest model [8], where polymer chains are represented by sequences of N_{ch} beads each. The beads interact via a bonded potential (FENE springs) in order to ensure connectivity, and a non-bonded potential to model the excluded volume effect as well as the quality of the solvent. In good solvent, the latter interaction is simply a purely repulsive Lennard-Jones (LJ) potential. For the form of these potentials, as well as the parameters, see [8]. The LJ potential also defines the unit system of the simulation (each bead has unit mass). The effects of less-than-perfect or even poor solvent quality are modeled by adding an attractive tail to the non-bonded pair interaction. For this tail, we take a suitably fitted cosine wave such that the range of the potential is 1.5 and its depth a parameter $\phi_{attr} \geq 0$, which is a direct measure of solvent quality. For details of that potential, see [17]. This system is simulated by Molecular Dynamics (MD) and at the same time coupled to a standard D3Q19 Lattice Boltzmann (LB) model. The latter represents the momentum transport through the solvent and has the thermodynamic properties of an ideal gas. The coupling is facilitated by a Stokes friction acting on each bead. The dissipative nature of the coupling ensures that it does not alter the thermodynamics of the polymer system. Both MD and LB are supplemented by a Langevin thermal noise such that the temperature is being kept constant. For technical details of that approach, as well as the underlying theory, see [5]. It should be noted that the simulations are done in three-dimensional space,

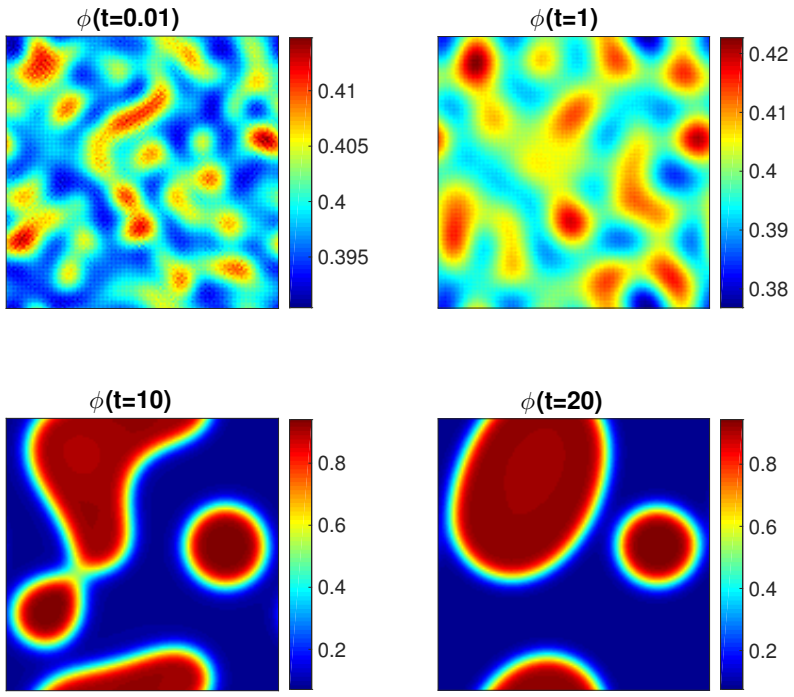

Fig. 1 128×128 grid with homogeneous initial volume fraction with noise: $\phi(t=0) = 0.4 + \delta, \quad \delta \in [-0.05, 0.05]$.

while the solution of the macroscopic equations is done in 2D. The pure LB fluid is strictly Newtonian, and all non-Newtonian effects arise from the coupling to the polymer system.

5 Numerical Experiments

As a first numerical experiment, the dynamic equations were solved on our computational domain $\Omega = [0,1] \times [0,1]$, which is devided into 128×128 grid cells and has periodic boundaries. The initial data of the volume fraction $\phi(t=0)$ is taken to be constant with a small random perturbation and the initial velocity and bulk stress are set to zero. The elastic stress tensor $\sigma(t=0) = \sqrt{2}\mathbb{1}$, the mixing constant $C_0 = 1/600$, the molecular weights $n_p = n_s = 1$, the Flory constant $\chi_0 = 3.3$ and the temperature $T = 1.1$. Furthermore the mobility coefficient $M = 10$ and the relaxation coefficients $\tau^0 = 10, \tau_s^0 = 5$ and $m_s^0 = 0.2$. The experiment as shown in Figure 1 demonstrates phase separation by aggregation of polymer molecules towards droplets. The droplets merge over time causing noticeable decreases of the

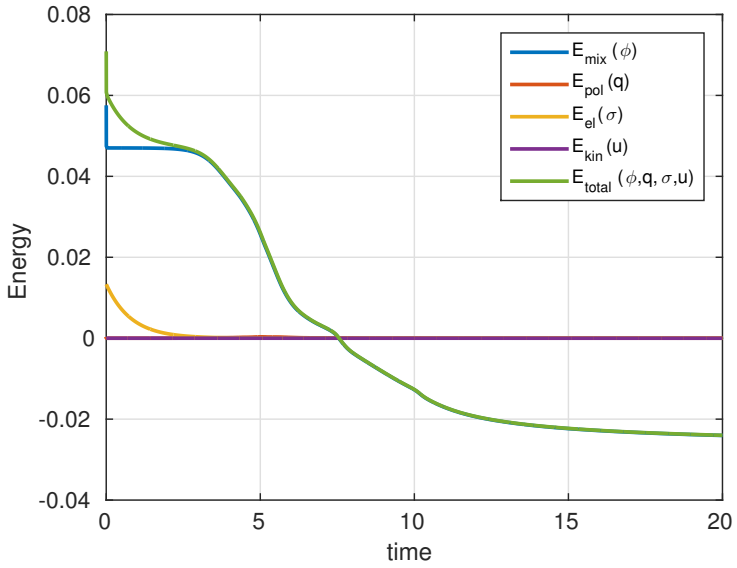

Fig. 2 Energy evolution in experiment 1.

mixing energy, as shown in Figure 2. Accordant to our proofs, the total energy is (strictly) monotonically decreasing over time, even while there is no merging, which is related to the surface minimization of the droplets.

As a second numerical experiment, we ran the LB/MD system for the following parameters: We study 40 chains of 100 beads each immersed in a volume of size 80^3, such that the volume fraction is roughly 4×10^{-3}, assuming a bead diameter of one LJ unit. The system is equilibrated in good solvent conditions ($\phi_{attr} = 0$) at temperature $T = 1$ (in units where Boltzmann's constant is one). Coupling to the LB system is facilitated by a Stokes friction $\zeta = 20$ and nearest-neighbor velocity interpolation. The MD time step is 5×10^{-3} and the LB time step ten times larger. The LB lattice spacing is one, and the LB shear viscosity is four. After equilibration ϕ_{attr} is suddenly increased to one, which is in the poor-solvent regime. Figure 3, left column, shows the time development of the system after this "quench".

The starting configuration of the 3D simulation was then transferred to the 2D solver of the macroscopic equations by subdividing the 3D system into columns of size $1 \times 1 \times 80$, counting the number of beads in each column and averaging their velocities weighted with the solvent velocity field. By such a projection we obtain an effective 2D volume fraction, which is, on average, roughly 0.3 and an effective 2D velocity field. Further parameters of the macroscopic solver are unchanged.

The numerical scheme (right column in Fig. 3) behaves analogous to the first experiment. Starting with initial configuration (at the top) the polymer concentration is then being smoothed (middle) and the system starts to phase-separate by aggregation into larger droplets (bottom). The 3D MD/LB simulations (left column

in Fig. 3) demonstrate a similar process with another level of details. The polymer chains in the initial configuration at good solvent condition form coils (top). After quenching the system into poor solvent regime the individual chains collapse (middle) and later form larger droplets by aggregation (bottom).

Although the mapping is of course extremely crude, it is nevertheless clear that the two systems evolve at least somewhat similarly. The relations for mass and energy scales between two models can be established by matching volume fractions and Flory parameters. However, a detailed comparison of time scales has not yet been accomplished: Though the viscosity of the fluid in the numerical model is known, at least a tiny fraction of the polymer is always present in every grid cell. Only averaging over these cells will give us the desired value of the effective viscosity needed to match the time scales. This analysis is left for future work.

6 Outlook

The present work is intended only as a first step towards much more detailed investigations. It is hoped on the one hand that in the future the underlying physics of the dynamic equations will become more clear, and on the other hand that much more detailed and stringent comparisons will provide deeper insight and perhaps also the development of more refined and accurate macroscopic models, with the possible perspective of even constructing multiscale models, which would consist of hybrid schemes that incorporate aspects of both the approaches presented here.

References

1. Abels, H., Depner, D., Garcke, H.: Existence of weak solutions for a diffuse interface model for two-phase flows of incompressible fluids with different densities. Journal of Mathematical Fluid Mechanics **15**(3), 453–480 (2013). DOI 10.1007/s00021-012-0118-x
2. Barrett, J.W., Boyaval, S.: Existence and approximation of a (regularized) Oldroyd-B model. Mathematical Models and Methods in Applied Sciences **21**(09), 1783–1837 (2011). DOI 10.1142/S0218202511005581
3. Bray, A.J.: Theory of phase-ordering kinetics. Advances in Physics **51**(2), 481–587 (2002). DOI 10.1080/00018730110117433
4. Cheng, Y., Kurganov, A., Qu, Z., Tang, T.: Fast and stable explicit operator splitting methods for phase-field models. Journal of Computational Physics **303**, 45–65 (2015). DOI 10.1016/j.jcp.2015.09.005
5. Dünweg, B., Ladd, A.J.C.: Lattice Boltzmann simulations of Soft Matter systems. In: C. Holm, K. Kremer (eds.) Advanced Computer Simulation Approaches for Soft Matter Sciences III, no. 221 in Advances in Polymer Science, pp. 89–166. Springer Berlin Heidelberg (2009)
6. Fattal, R., Kupferman, R.: Time-dependent simulation of viscoelastic flows at high Weissenberg number using the log-conformation representation. Journal of Non-Newtonian Fluid Mechanics **126**(1), 23–37 (2005). DOI 10.1016/j.jnnfm.2004.12.003

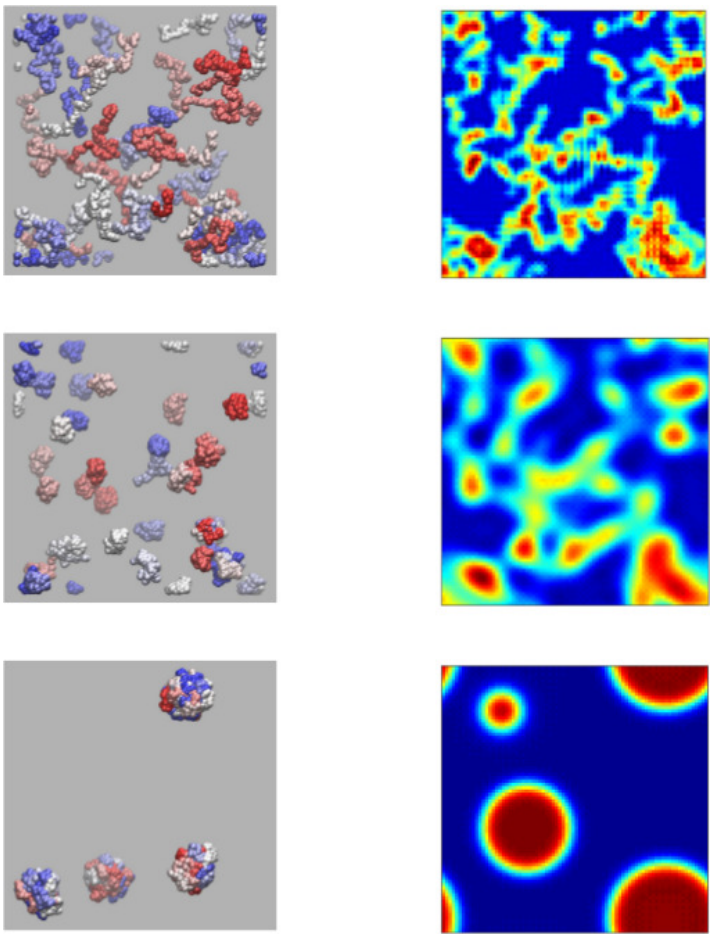

Fig. 3 80^3 Lattice Boltzmann solvent cube with polymer chains from Molecular Dynamics (first row, left column) mapped to 80×80 2D grid and solved with our numerical scheme (right column).

7. Fernández-Cara, E., Guillén-González, F.M., Ortega, R.R.: Mathematical modeling and analysis of viscoelastic fluids of the Oldroyd kind. In: Handbook of numerical analysis (volume VIII), pp. 543–660. Elsevier (2002)
8. Grest, G.S., Kremer, K.: Molecular dynamics simulation for polymers in the presence of a heat bath. Physical Review A **33**(5), 3628–3631 (1986). DOI 10.1103/PhysRevA.33.3628
9. Guillén-González, F., Tierra, G.: On linear schemes for a Cahn-Hilliard diffuse interface model. Journal of Computational Physics **234**, 140–171 (2013). DOI 10.1016/j.jcp.2012.09.020
10. Hohenberg, P.C., Halperin, B.I.: Theory of dynamic critical phenomena. Reviews of Modern Physics **49**(3), 435–479 (1977). DOI 10.1103/RevModPhys.49.435
11. Hu, D., Lelièvre, T.: New entropy estimates for the Oldroyd-B model and related models. Communications in Mathematical Sciences **5**(4), 909–916 (2007)

12. Kay, D., Welford, R.: Efficient numerical solution of Cahn-Hilliard-Navier-Stokes fluids in 2d. SIAM Journal on Scientific Computing **29**(6), 2241–2257 (2007). DOI 10.1137/050648110
13. Lee, D., Huh, J.Y., Jeong, D., Shin, J., Yun, A., Kim, J.: Physical, mathematical, and numerical derivations of the Cahn-Hilliard equation. Computational Materials Science **81**, 216–225 (2014). DOI 10.1016/j.commatsci.2013.08.027
14. Lukáčová-Medviďová, M., Notsu, H., She, B.: Energy dissipative characteristic schemes for the diffusive Oldroyd-B viscoelastic fluid. International Journal for Numerical Methods in Fluids **81**(9), 523–557 (2016). DOI 10.1002/fld.4195
15. Onuki, A.: Phase transition dynamics. Cambridge University Press (2002)
16. Rubinstein, M., Colby, R.H.: Polymer physics. Oxford University Press, Oxford; New York (2003)
17. Soddemann, T., Dünweg, B., Kremer, K.: A generic computer model for amphiphilic systems. The European Physical Journal E **6**(1), 409–419 (2001). DOI 10.1007/s10189-001-8054-4
18. Tanaka, H.: Viscoelastic phase separation. Journal of Physics: Condensed Matter **12**(15), R207 (2000). DOI 10.1088/0953-8984/12/15/201
19. Tierra, G., Guillén-González, F.: Numerical methods for solving the Cahn-Hilliard equation and its applicability to related energy-based models. Archives of Computational Methods in Engineering **22**(2), 269–289 (2015). DOI 10.1007/s11831-014-9112-1
20. Turek, S., Ouazzi, A., Hron, J.: On pressure separation algorithms (PSepA) for improving the accuracy of incompressible flow simulations. International Journal for Numerical Methods in Fluids **59**(4), 387–403 (2009). DOI 10.1002/fld.1820
21. Zhou, D., Zhang, P., E, W.: Modified models of polymer phase separation. Physical Review E **73**(6), 061,801 (2006). DOI 10.1103/PhysRevE.73.061801